Article

Enhancement of Visual Field Predictions with Pointwise Exponential Regression (PER) and Pointwise Linear Regression (PLR)

Esteban Morales[1], John Mark S. de Leon[1], Niloufar Abdollahi[1], Fei Yu[1,2], Kouros Nouri-Mahdavi[1], and Joseph Caprioli[1]

[1] The Jules Stein Eye Institute, David Geffen School of Medicine at UCLA, Los Angeles, CA, USA
[2] Department of Biostatistics and Epidemiology, Jonathan and Karin Fielding School of Public Health at UCLA, Los Angeles, CA, USA

Purpose: The study was conducted to evaluate threshold smoothing algorithms to enhance prediction of the rates of visual field (VF) worsening in glaucoma.

Methods: We studied 798 patients with primary open-angle glaucoma and 6 or more years of follow-up who underwent 8 or more VF examinations. Thresholds at each VF location for the first 4 years or first half of the follow-up time (whichever was greater) were smoothed with clusters defined by the nearest neighbor (NN), Garway-Heath, Glaucoma Hemifield Test (GHT), and weighting by the correlation of rates at all other VF locations. Thresholds were regressed with a pointwise exponential regression (PER) model and a pointwise linear regression (PLR) model. Smaller root mean square error (RMSE) values of the differences between the observed and the predicted thresholds at last two follow-ups indicated better model predictions.

Results: The mean (SD) follow-up times for the smoothing and prediction phase were 5.3 (1.5) and 10.5 (3.9) years. The mean RMSE values for the PER and PLR models were unsmoothed data, 6.09 and 6.55; NN, 3.40 and 3.42; Garway-Heath, 3.47 and 3.48; GHT, 3.57 and 3.74; and correlation of rates, 3.59 and 3.64.

Conclusions: Smoothed VF data predicted better than unsmoothed data. Nearest neighbor provided the best predictions; PER also predicted consistently more accurately than PLR. Smoothing algorithms should be used when forecasting VF results with PER or PLR.

Translational Relevance: The application of smoothing algorithms on VF data can improve forecasting in VF points to assist in treatment decisions.

Introduction

Glaucoma is an optic neuropathy characterized by progressive functional and structural deterioration.[1] The ability of clinicians to accurately estimate rates of functional decline with visual fields (VF) is an important basis for making management decisions.[2] Because of the confounding effect of variability between VF tests and the inherent lack of external validation, several prediction techniques have been developed.[3,4] Visual field indices that consider sensitivity at individual locations are more sensitive to change than global VF indices.[5,6] Measurement of glaucoma decay rates helps identify fast progressing patients who may need more aggressive treatment to lessen their chances of visual disability, as opposed to slower progressing patients who may be spared the costs and morbidity of treatment.[7]

Exponential and linear models have been used to fit and predict visual field behavior. The exponential model assumes a constant multiplicative rate of change while the linear model assumes a constant additive rate of change. A validated pointwise exponential regression (PER) technique has been described recently[2,8] and measures visual decay rates of all locations of the VF across a wide spectrum of disease severity. Pointwise exponential regression was used to partition VF points into fast and slow components; it was observed that the faster progressing points clustered in a pattern consistent with the anatomy of the retinal nerve fiber layer (RNFL).[8]

Recent studies demonstrated that VF cluster analysis, as opposed to individual test locations, dampens the effects of longitudinal VF variability,[9] facilitates the identification of early glaucomatous damage,[9–11] and increases the specificity of glaucoma diagnosis.[12]

A strategy to reduce VF measurement variability without additional testing or the exclusion of unreliable tests is post hoc application of a spatial filters to VF data.[13,14] Spatial filtering, a technique used commonly in digital image processing, can smooth the data and reduce the noise by applying mathematical processes that exploit the spatial relationship between neighboring numeric values.[14] As the VF is a numerical matrix, the same rationale may be applied to VF data. With this approach, the measured threshold sensitivity of each test location within the VF is replaced by a "weighted" value, which is estimated with neighboring sensitivity values.[15]

The aim of this study was to enhance VF forecasting with PER and PLR models by investigating four different smoothing algorithms based on spatial clustering. We hypothesized that such an approach may improve the VF signal-to-noise ratio and enhance predictions of VF behavior.

Methods

Patients

A total of 798 eyes of 588 patients from two cohorts was available for the study and represented a wide spectrum of glaucoma severity. The first cohort included 409 eyes of 279 University of California, Los Angeles (UCLA) patients diagnosed with primary open-angle glaucoma (POAG). The second cohort included 389 eyes of 309 Advanced Glaucoma Intervention Study (AGIS) patients. The AGIS study design and methods have been described in detail previously.[16,17] Tests were performed with the Humphrey VF analyzer (Carl Zeiss Ophthalmic Systems, Inc., Dublin, CA) with a 24-2 test pattern, size III white stimulus, and with either the full threshold strategy or the ad Swedish Interactive Threshold Algorithm (SITA) Standard strategy. The 24-2 test pattern recorded sensitivities from 54 points of the VF including the physiological blind spot.

Additional inclusion criteria for eyes in the study are: eyes with adequate VF reliability defined as having <30% fixation loss, false-positive and false-negative response rates, and eyes with 6 or more years of follow-up that underwent 8 or more VF

examinations. Each eye's VF series contained either all SITA or all full threshold examinations; the algorithms were not mixed for any eye, nor were they based on a decision made by the examiner. This study was approved by the UCLA Human Research Protection Program, was performed in accordance with the tenets set forth in the Declaration of Helsinki, and complied with Health Insurance Portability and Accountability Act (HIPAA) regulations.

VF Location Clustering

Each of the 54 VF points were grouped as clusters defined by the following four models: (1) a nearest neighbor weighting model (NN), (2) the Garway-Heath model,[1] (3) the glaucoma hemi-field test model (GHT),[18] and (4) a correlation of rates[19] model. The raw sensitivity values (dB) at each VF location for the first 4 years or the first half of the follow-up time (whichever was greater) were weighted individually based on distance influences from each of the other locations for each of the four models.

VF Clustering models ([Fig. 1])

NN Model

In this model the sensitivity of each point was weighted based on distance and sensitivity of adjacent neighboring points. The minimum number of possible neighbors was 4 and the maximum number of possible neighbors was 8.

Garway-Heath Model

Garway-Heath et al.[1] defined six VF clusters based on the structure–function correlations between RNFL bundle defects on fundus photographs and VF defects observed in a group of normal-tension glaucoma patients.

GHT Model

The 54 VF test locations were divided into 10 GHT clusters corresponding to RNFL anatomy as described by Asman and Heijl.[18] There were five clusters in the superior hemifield and five mirror-image clusters in the inferior hemifield.

Correlation of Rates Model

This weighting model was based on the correlation of longitudinal rates of decay at each VF test locations with all the other VF test locations using hierarchical cluster analysis. It was shown that correlated rates of change, in patients with glaucoma,
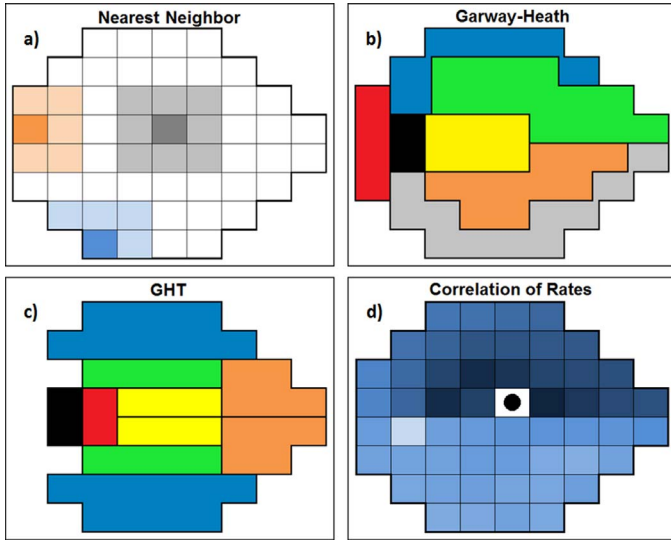
Figure 1. Visual representation of the four clustering techniques used for smoothing. (a) Nearest neighbor weighted the sensitivity of each point based on distance and sensitivity of adjacent neighboring points; three examples of nearest neighbor locations are shown. (b) Garway-Heath defined six visual field clusters based on structure-function correlations between RNFL bundle defects on fundus photographs and VF defects observed in a group of normal-tension glaucoma patients. (c) GHT defined 10 clusters corresponding to RNFL anatomy. (d) Correlation of rates uses correlation of longitudinal rates of decay at each VF test locations with all the other VF test locations using hierarchical cluster analysis; one location's (*solid circle* near fixation above *horizontal*) color scale representation of its correlation of rates is shown.

cluster into regions consistent with RNFL bundle patterns.[19]

Distance Weighting and Correlation Weighting

Calculating the smoothed VF locations based on distance was defined as:

$$\text{Weighted Location} = (VF_{\text{Location}})\frac{1}{2} + \frac{1}{2}\left[\frac{\sum_1^n (w \times VF_{\text{Neighbor}})}{\sum_1^n (w)}\right],$$

where d = distance = 1 (for adjacent VF locations), w = weight = $1/d^2$, n = number of neighboring VF locations, VF_{Location} = dB value of VF location being weighted, and VF_{Neighbor} = dB value of neighboring VF location.

Calculating the smoothed VF locations based on the correlation of rates was defined as:

Correlation of Rates Weighted Location

$$= (VF_{\text{Location}})\frac{1}{2} + \frac{1}{2}\left[\frac{\sum_1^n (c \times VF_{\text{Neighbor}})}{\sum_1^n (c)}\right],$$

where c = correlation value. The final follow-up for the smoothed locations required at least two years' duration from the first follow-up to be predicted.

VF Regression and Prediction

The two test locations at the physiological blind spot and the locations at which the first three initial measurements were zero dB were excluded from the regression analysis. The raw and cluster-weighted (smoothed) 54 VF point sensitivities in decibels (dB) were regressed with PER and PLR for the first four years or half of the follow-up time (whichever was greater) and regression coefficients were obtained. The mathematical models used in the regressions were:

1. PER: $y = e^{\alpha+\beta x}$, or equivalently, $ln(y) = \alpha + \beta x$
2. PLR: $y = \alpha + \beta x$

The variable y represents threshold sensitivity in dB and x represents follow-up time in years. The variables α and β are parameters estimated by the models, where α is the intercept and β is the regression coefficient.

Regression curves, representing pointwise decay, for each model were created from these coefficients for the smoothed and unsmoothed VF locations. These curves were used to predict the sensitivity (dB) of the last follow-up visit and were compared to the observed VF sensitivity (average of the final two follow-up visits). The root mean square errors (RMSE) of the difference of the predicted and observed sensitivities were calculated. This was done for the smoothed clustered (4 prediction models) locations and the raw nonclustered locations.

$$\text{RMSE} = \sqrt{\frac{\sum_{i=1}^n (X_{\text{obs},i} - X_{\text{model},i})^2}{n}},$$

where X_{obs} = average sensitivity (dB) of the final 2 follow-up visits of the observed points, X_{model} = predicted sensitivity (dB) of the last follow-up of the smoothed points, n = number of visual field points, and i = eye.

Only locations with a negative regression coefficient were predicted. The linear model predictions

Table 1. Patient Demographics and VF Series Characteristics

Eyes, *n*	603
Patients, *n*	473
Mean age ± SD, y	68.8 ± 11.4
Mean smoothed follow-up ± SD, y	5.3 ± 1.5
Mean smoothed VFs ± SD, *n*	10.5 ± 3.9
Mean total VF follow-up ± SD, y	10.8 ± 3.4
Mean total VFs ± SD	18.9 ± 7.0

were censored at 0 dB. The model with the best predictive ability was assessed with values of RMSE. Since there is no formal statistical test to determine the level of significance between models, the RMSE of the models were ranked from the lowest to highest. The model with the lowest RMSE was considered the best predictor of the observed final sensitivity. All statistical analyses were done in the open source programming language R.[20]

Results

Patient Data

We included in the study 603 eyes of 473 patients with POAG (6932 VF locations). The mean (±SD) duration and number of VFs used to construct the prediction were 5.3 (±1.5) and 10.5 (±3.9) years, respectively. The mean (±SD) total duration and number of VFs were 10.8 (±3.4) years and 18.9 (±7.0), respectively (Table 1). The VF test strategies for the UCLA group included SITA standard (88%) and full threshold (12%) exams. The VF test strategies for the AGIS group were all full threshold exams.

Prediction and RMS

The mean RMSE values of the differences between the observed and the predicted thresholds at last

follow-up for each VF location for the PER were 6.09 dB for the unsmoothed data, 3.40 dB for NN, 3.47 dB for the Garway-Heath clusters, 3.57 dB for GHT, and 3.59 dB for the correlation of rates (Table 2).

The mean RMSE values of the differences between the observed and predicted thresholds at last follow-up for each VF location for the PLR were 6.55 dB for the unsmoothed data, 3.42 dB for NN, 3.48 dB for the Garway-Heath clusters, 3.74 dB for GHT, and 3.64 dB for the correlation of rates (Table 2).

Absolute differences in the sensitivity (dB) between the smoothed and observed values for each of the four models are shown in Figure 2. All *P* values between the smoothed and unsmoothed differences in sensitivities were $P < 0.001$. The resultant RMSE values ranked from lowest to highest (dB) are shown in Table 2.

Discussion

The smoothing algorithms enhanced the predictive ability of the PER and PLR models by integrating weighted spatial contributions from neighboring VF test locations within the specific cluster. Although differences between the VF PER and PLR predictions with the four smoothing models and the raw predictions were not large, the NN had the lowest RMSE for the exponential and linear models (Table

Table 2. Comparison of the RMSE Values of the Difference Between the Observed and Predicted Threshold for PER and PLR Models

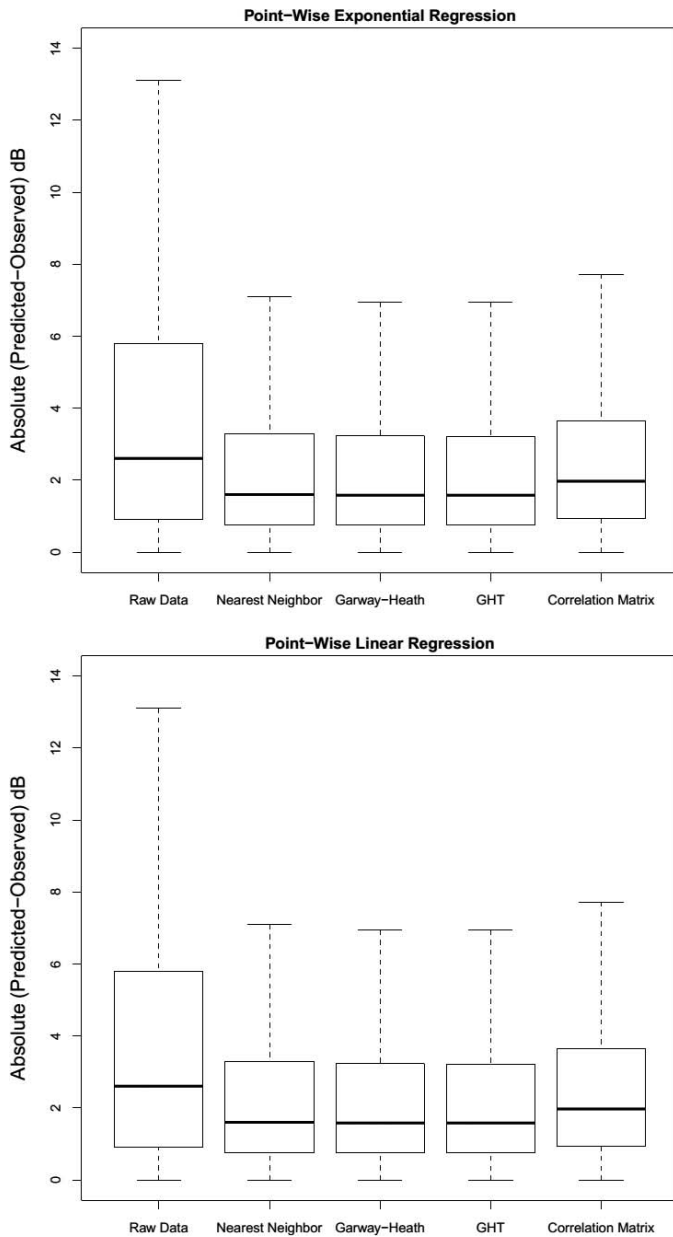|	Exponential		Linear	
	RMSE, dB	Average, dB[a]	RMSE, dB	Average, dB[a]
Raw data	6.09	4.13	6.55	4.42
Nearest neighbor	3.40	2.41	3.42	2.39
Garway heath	3.47	2.42	3.48	2.40
GHT	3.57	2.45	3.74	2.52
Correlation matrix	3.59	2.67	3.64	2.64

[a] Absolute (predicted − observed).

Figure 2. Absolute differences in the sensitivity (dB) between the smoothed and observed values per cluster model for PER and PLR models. Outliers have been removed from the graph.

2) and, thus, provided the most favorable predictions. The boxplots of the absolute difference of the predicted and observed for each smoothing algorithm are comparatively shorter than the boxplot for the raw data (Fig. 2). There is a larger spread in the absolute difference of the predicted and observed for the raw data. The use of the unsmoothed, raw VF location values yielded the least accurate predictions (highest RMSE values) for the exponential and linear models. Analysis of variance (ANOVA) with random

effects was used to compare all four smoothing techniques and the raw data; the result was significant for PER and PLR ($P < 0.001$). An ANOVA with random effects also was used to compare all four smoothing techniques excluding the raw data, and the result also was significant for PER and PLR ($P < 0.001$). While the means among the four smoothing techniques are significantly different, due to the large sample size, the clinical significance between the smoothing techniques is admittedly marginal.

The relationship among test locations across the VF has been the subject of many studies, some suggesting that clustering is essential for early detection of damage in glaucoma,[9–11] and others observed that clusters are correlated to the optic nerve head[1] and RNFL anatomy.[19,21] Clustering of abnormal VF points in an arcuate pattern is more specific for glaucoma rather than if the abnormal points are scattered.[12] Requiring progressing points to belong to the same GHT cluster increases the specificity to recognize significant change.[22] Traditional progression analysis techniques, such as pointwise linear regression (PLR) or glaucoma probability analysis (GPA), do not nominally require individual progressing points to belong to a specific cluster.

It has been suggested that using change in a single location as a criterion for progression leads to high false-positive rates, and that assessing fields with a cluster-based approach enhances specificity.[19,22,23] Mandava et al.,[9] with 11 clusters in a set of 76 Octopus program G1 VFs, reported that VF cluster analysis performed better than global indices (mean defect or MD) for the detection of localized VF progression and had less long-term VF fluctuation compared to pointwise analyses. The clustered MDs had a sensitivity of 90% and a specificity of 93% while the global MD had a sensitivity of 81% and a specificity of 91%. The authors observed that cluster analysis was effective in detecting localized loss and in dampening long-term fluctuation, and pointed out the use of clusters to distinguish normal from glaucomatous as well as stable from deteriorating VFs.

Another study introduced a novel clustering method consistent with RNFL anatomy and showed improved detection and prediction of progression with correlated pointwise rates of decay.[19] Various mapping and clustering techniques[1,10,21,24–26] have been designed with a variety of algorithms. These techniques also established relationships between functional and structural glaucoma changes and attempted to elucidate this relationship objectively, particularly with regard to VF progression. The use of

customized perimetric maps has been reported recently.[27] Spatial averaging with the use of such customized maps may provide additional benefits to enhance the accuracy of predicted VF sensitivities, and should be investigated.

Our results showed that PER and PLR coupled with any of the four smoothing models provided more accurate predictions of future VF behavior than was achieved with the unsmoothed VF sensitivities. Based on the RMSE (Table 2), the four smoothing algorithms, as compared to raw or unsmoothed data, likely improved the VF signal-to-noise ratio, and provided more accurate predictions. We initially expected that the NN model would be least predictive versus the others, given its lack of anatomical basis; however, it provided the best VF predictions, probably solely due to lowering variability through strictly localized averaging.[9]

One limitation of this study was the VF algorithms used by the 2 cohorts were not uniform (full threshold and SITA standard algorithms were used), though never mixed in the same series; we then would consider these results a "worst-case scenario." However, one study showed no difference in the generated MD values between full threshold and SITA standard algorithms.[28] The differences in RMSE and absolute dB values between the techniques was small, so that the clinical relevance between the smoothing techniques is limited; still, improvements to VF variability and prediction should be incorporated in clinical research whenever possible.

In summary, among glaucoma patients with a wide spectrum of severities, application of smoothing algorithms to PER and PLR models improved prediction of VF behavior compared to the use of raw data. Although the differences among the VF PER and PLR predictions among the four smoothing algorithms and raw predictions is small, all performed considerably better than the unsmoothed data. The best predictions were provided by NN; PER also predicted consistently more accurately than did PLR. Smoothing algorithms should be used when forecasting VF results with PER or PLR. Such enhancements of VF analyses, by more accurately approximating the rates of worsening glaucoma patients, improve VF progression predictions and may assist the identification of fast progressors, so that appropriate treatments can be applied to lessen their chances for visual disability.

References

1. Garway-Heath DF, Poinoosawmy D, Fitzke FW, Hitchings RA. Mapping the visual field to the optic disc in normal tension glaucoma eyes. *Ophthalmology*. 2000;107:1809–1815.
2. Azarbod P, Mock D, Bitrian E, et al. Validation of point-wise exponential regression to measure the decay rates of glaucomatous visual fields. *Invest Ophthalmol Vis Sci*. 2012;53:5403–5409.
3. Werner EB, Bishop KI, Koelle J, et al. A comparison of experienced clinical observers and statistical tests in detection of progressive visual field loss in glaucoma using automated perimetry. *Arch Ophthalmol*. 1988;106:619–623.
4. Katz J, Congdon N, Friedman DS. Methodological variations in estimating apparent progressive visual field loss in clinical trials of glaucoma treatment. *Arch Ophthalmol*. 1999;117:1137–1142.
5. Wild JM, Hussey MK, Flanagan JG, Trope GE. Pointwise topographical and longitudinal modeling of the visual field in glaucoma. *Invest Ophthalmol Vis Sci*. 1993;34:1907–1916.
6. Chauhan BC, Drance SM, Douglas GR. The use of visual field indices in detecting changes in the visual field in glaucoma. *Invest Ophthalmol Vis Sci*. 1990;31:512–520.
7. Caprioli J. The importance of rates in glaucoma. *Am J Ophthalmol*. 2008;145:191–192.
8. Caprioli J, Mock D, Bitrian E, et al. A method to measure and predict rates of regional visual field decay in glaucoma. *Invest Ophthalmol Vis Sci*. 2011;52:4765–4773.
9. Mandava S, Zulauf M, Zeyen T, Caprioli J. An evaluation of clusters in the glaucomatous visual field. *Am J Ophthalmol*. 1993;116:684–691.
10. Chauhan BC, Drance SM, Lai C. A cluster analysis for threshold perimetry. *Graefes Arch Clin Exp Ophthalmol*. 1989;227:216–220.
11. Katz J, Sommer A, Gaasterland DE, Anderson DR. Comparison of analytic algorithms for detecting glaucomatous visual field loss. *Arch Ophthalmol*. 1991;109:1684–1689.

translational vision science & technology

12. Asman P, Heijl A. Arcuate cluster analysis in glaucoma perimetry. *J Glaucoma*. 1993;2:13–20.
13. Fitzke FW, Crabb DP, McNaught AI, Edgar DF, Hitchings RA. Image processing of computerised visual field data. *Br J Ophthalmol*. 1995;79:207–212.
14. Crabb DP, Fitzke FW, McNaught AI, Edgar DF, Hitchings RA. Improving the prediction of visual field progression in glaucoma using spatial processing. *Ophthalmology*. 1997;104:517–524.
15. Strouthidis NG, Scott A, Viswanathan AC, Crabb DP, Garway-Heath DF. Monitoring glaucomatous visual field progression: the effect of a novel spatial filter. *Invest Ophthalmol Vis Sci*. 2007;48:251–257.
16. Ederer F, Gaasterland DE, Sullivan EK, Investigators. AGIS. The Advanced Glaucoma Intervention Study (AGIS): 1. Study design and methods and baseline characteristics of study patients. *Control Clin Trials*. 1994;15:299–325.
17. The Advanced Glaucoma Intervention Study (AGIS): 4. Comparison of treatment outcomes within race. Seven-year results. *Ophthalmology*. 1998;105:1146–1164.
18. Asman P, Heijl A. Glaucoma Hemifield Test. Automated visual field evaluation. *Arch Ophthalmol*. 1992;110:812–819.
19. Nouri-Mahdavi K, Mock D, Hosseini H, et al. Pointwise rates of visual field progression cluster according to retinal nerve fiber layer bundles. *Invest Ophthalmol Vis Sci*. 2012;53:2390–2394.
20. R Core Team R: A language and environment for statistical computing. *R Found Stat Comput Vienna Austria*. 2013. Available at: http://www.R-project.org/.
21. Asaoka R, Russell RA, Malik R, Crabb DP, Garway-Heath DF. A novel distribution of visual field test points to improve the correlation between structure-function measurements. *Invest Ophthalmol Vis Sci*. 2012;53:8396–8404.
22. Nouri-Mahdavi K, Caprioli J, Coleman AL, Hoffman D, Gaasterland D. Pointwise linear regression for evaluation of visual field outcomes and comparison with the advanced glaucoma intervention study methods. *Arch Ophthalmol*. 2005;123:193–199.
23. Heijl A, Bengtsson B, Lindgren G. Visual field progression in glaucoma. *Br J Ophthalmol*. 1998;82:1097–1098.
24. Ferreras A, Pablo LE, Garway-Heath DF, Fogagnolo P, García-Feijoo J. Mapping standard automated perimetry to the peripapillary retinal nerve fiber layer in glaucoma. *Invest Ophthalmol Vis Sci*. 2008;49:3018–3025.
25. Zhang X, Raza AS, Hood DC. Detecting glaucoma with visual fields derived from frequency-domain optical coherence tomography. *Invest Ophthalmol Vis Sci*. 2013;54:3289–3296.
26. Nilforushan N, Nassiri N, Moghimi S, et al. Structure-function relationships between spectral-domain OCT and standard achromatic perimetry. *Invest Ophthalmol Vis Sci*. 2012;53:2740–2748.
27. Ballae Ganeshrao S, Turpin A, Denniss J, McKendrick AM. Enhancing structure–function correlations in glaucoma with customized spatial mapping. *Ophthalmology*. 2015;122:1–11.
28. Demirel S, De Moraes CGV, Gardiner SK, et al. The rate of visual field change in the ocular hypertension treatment study. *Invest Ophthalmol Vis Sci*. 2012;53:224–227.

translational vision science & technology